(9) The relationship between the triplet lifetime, triplet energy migration constant, and distribution of pair separations to the form of the delayed fluorescence decay function is somewhat subtle and is the subject of ongoing research (Webber, S. E., unpublished results).
(10) Schnabel, W. *Makromol. Chem.* **1979**, *180*, 1487.
(11) Das, P. K.; Sciano, J. C. *Macromolecules* **1981**, *14*, 693.
(12) Utracki, L. A.; Simha, R. *Makromol. Chem.* **1968**, *117*, 94.
(13) Wagner, P. J. *J. Am. Chem. Soc.* **1967**, *89*, 2820.
(14) Wagner, P. J. *Mol. Photochem.* **1969**, *1*, 71.
(15) It has been found by Wagner[13,14] that triplet benzophenone does not sensitize biphenyl at a diffusion-limited rate in fluid solution. Wagner[14] estimated that the triplet energy of the nonvertical transition was approximately 1 kcal less than triplet energy of benzophenone. From our other work with P4VBP[5] we estimated the triplet-state energy of the biphenyl pendant group as 67 kcal/mol, or 2 kcal/mol lower than benzophenone. While the benzophenone triplet is a very efficient sensitizer, the bimolecular rate constant for biphenyl sensitization is less than diffusion limited.

Interpretation of Electronic Energy Transport Experiments in Polymeric Systems

Glenn H. Fredrickson and Curtis W. Frank*

Department of Chemical Engineering, Stanford University, Stanford, California 94305.
Received October 27, 1982

ABSTRACT: The theoretical foundation for the interpretation of transient and photostationary fluorescence experiments in the presence of electronic energy transport is reviewed. Transient trapping experiments are described for both uniform and nonuniform disordered media by the decay of $G^D(t)$, the integrated average density of donor excitations. Furthermore, the photostationary-state observables are directly related to the Laplace transform of $G^D(t)$. Expressions are collected for $G^D(t)$ that can be applied to homogeneous systems of donors and traps exhibiting direct or migration-assisted trapping. Similarly, transient fluorescence depolarization experiments can be described by $G^S(t)$, the ensemble-averaged, initial site excitation probability, while photostationary depolarization is interpreted in terms of the Laplace transform of $G^S(t)$. Useful expressions are obtained for the photostationary-state ratio of trap to donor intensities, a nondiffusive "effective migration length", and the steady-state anisotropy. The importance of homogeneity, dimensionality, and proper transition moment averaging is discussed for polymeric and nonpolymeric systems. Finally, the utility of the theory reviewed in this paper is illustrated with several sets of trapping and depolarization data found in the polymer literature.

I. Introduction

The use of fluorescence probes for the characterization of polymer morphology has become widespread in recent years.[1,2] The technique of excimer fluorescence provides direct quantitative information on intra- and intermolecular interactions and has proved useful in the analysis of phase separation and compatibility of solid blends[3-6] and in the study of segmental rotation in solution.[7] Sensitization experiments have been used in polymers and biopolymers to measure intramolecular distances and also to characterize unknown chromophore distributions.[2] Fluorescence depolarization experiments yield useful information on conformational dynamics in solution[8] and furnish a measure of overall coil mobility.[9] Depolarization studies have also been used to characterize fluorescent copolymers, and they provide direct evidence for the presence of electronic energy migration in such systems.[10-17]

The transport and trapping of electronic excitations in polymeric materials is, in general, a very difficult many-body problem. Chromophores attached to polymer chains present an inhomogeneous medium for exciton transport processes. Such systems provide an anisotropic transport pathway with uncertain dimensionality and possibly a nonuniform distribution of transition moments. As a result, care must be taken in the selection of experimental systems and in the subsequent data analysis.

Recent theoretical advances in the treatment of energy migration and trapping in disordered, homogeneous systems have led to the conclusion that these transport processes are *nondiffusive* in nature.[18-25] Very accurate time-dependent solutions to the transport master equation have been obtained and connections made to experimental observables. In this paper we will attempt to review the recent theoretical developments for uniform systems and demonstrate how they can be applied to the analysis of experiments on macromolecules.

II. Trapping Theory

Trapping experiments generally involve the excitation of one type of chromophore, the donor or sensitizer, and the subsequent observation of the fluorescence from a second chromophore type, the trap, activator, or acceptor. The excitation energy can be directly transferred from the excited donor to a trap by a resonant or exchange mechanism[26] or may migrate via a similar mechanism to other donors from which direct trapping can take place. The transient excited donor and trap populations are intimately related to the distribution and concentration of both chromophore types and also to the interaction mechanism. In this paper only excitations that are transferred through a multipolar resonance mechanism will be considered, and the traps will be assumed to be "deep" or nondissociative.

The observables in both transient and photostationary trapping experiments can be directly connected with the donor excitation function, $G^D(t)$, which represents the probability that an excitation resides on a donor chromophore at time t in the absence of other decay processes. Since $G^D(t)$ is in general a nonexponential function, trapping kinetics cannot be described in terms of a trapping rate constant. However, a trapping rate *function* can be defined as[27]

$$k(t) = -\frac{d}{dt}[\ln G^D(t)] \tag{1}$$

so that the excited donor population obeys the equation

0024-9297/83/2216-1198$01.50/0

$$\frac{d}{dt}[D^*] = -k_D[D^*] - k(t)[D^*] \quad (2)$$

The rate constant, k_D, reflects the total rate of donor decay by radiative and nonradiative processes in the absence of energy transport.

In transient experiments with donors and nondissociative traps that emit radiatively, the fluorescence intensities can be expressed in terms of $G^D(t)$[27]

$$i_D(t) = q_{FD}k_D \exp(-k_D t)G^D(t) \quad (3a)$$

$$i_T(t) = q_{FT}k_T \exp(-k_T t)\int_0^t d\tau \exp(-k_D\tau)\left[-\frac{d}{d\tau}G^D(\tau)\right] \quad (3b)$$

In eq 3, k_D and k_T are the total rates of radiative and nonradiative decay of excited donors and traps, while q_{FD} and q_{FT} are the respective fluorescence quantum efficiencies.

Photostationary-state fluorescence data are often expressed in terms of the ratio of integrated trap to donor fluorescence intensities. The ratio is given by[27]

$$\frac{I_T}{I_D} = \frac{q_{FT}}{q_{FD}}\left[\frac{1-M}{M}\right] \quad (4)$$

where $1 - M$ is the trapping efficiency and M is related to $G^D(t)$ by

$$M = k_D\int_0^\infty dt \exp(-k_D t)G^D(t) \quad (5)$$

Since many transport models are formulated in terms of the Laplace transform of $G^D(t)$, it is useful to note that the photostationary results can be obtained directly from the expression

$$M = k_D\tilde{G}^D(s = k_D) \quad (6)$$

where the transform is defined by

$$\tilde{G}^D(s) = \int_0^\infty \exp(-st)G^D(t)\, dt \quad (7)$$

It should be emphasized that M is related to the time average of the nonexponential donor population and thus cannot be expressed in terms of a ratio of rate constants.[29]

The first analysis of the trapping problem was done by Förster.[30] An expression was developed for $G^D(t)$ when the excitations *cannot be transferred between donors* but when the energy can be directly transferred to a three-dimensional random distribution of traps by a dipole–dipole mechanism. The work has been extended to arbitrary dimensions and to isotropic, multipolar transport rates from donor to trap of the form

$$v(r) = k_D(R^{DT}/r)^s \quad (8)$$

The parameter s characterizes the order of the multipolar interaction, while the donor–trap interaction radius, R^{DT}, is the distance at which the transport rate equals k_D. The donor excitation function for this problem is given by[31-33]

$$G^D(t) = \exp\{-C_T\Gamma(1 - \Delta/s)(k_D t)^{\Delta/s}\}, \qquad s > \Delta \quad (9)$$

where the dimensionless trap concentration for a number density of trap chromophores, ρ_T, in Δ dimensions is defined by

$$C_T = V_\Delta(R^{DT})^\Delta\rho_T \quad (10)$$

and V_Δ is the volume of a unit sphere in Δ dimensions. $\Gamma(x)$ is the usual gamma function.

Equation 9 is applicable over a broad range of times and concentrations if donor–donor migration is negligible and if the surrounding medium is sufficiently nonviscous to allow transition moment randomization during the residence time of the excitation on the donor. However, the medium must also be viscous enough to prevent bulk chromophore diffusion from taking place on the time scale of the energy transport process.

In a highly viscous fluid or solid solution the isotropic rate defined in eq 8 is inappropriate. To determine $G^D(t)$ for such a system, it is necessary to perform a static average of transition moments for an orientation-dependent rate mechanism. For the special case of dipole–dipole ($s = 6$) transfer from a donor to randomly oriented acceptor dipoles in a rigid medium, the direct trapping result is

$$G^D(t) = \exp\{-\gamma_\Delta C_T\Gamma(1 - \Delta/6)(k_D t)^{\Delta/6}\} \quad (11)$$

where the orientation factor is given by

$$\gamma_1 = 0.8886, \quad 1\text{-D} \quad (12a)$$

$$\gamma_2 = 0.8468, \quad 2\text{-D} \quad (12b)$$

$$\gamma_3 = 0.8452, \quad 3\text{-D} \quad (12c)$$

Since we have not encountered the one- and two-dimensional results in the literature, the derivation of eq 11 is given in Appendix A. Comparison of eq 9 and 11 indicates that eq 9 can be taken as the general result for dipolar interactions if the replacement $C_T \rightarrow \gamma_\Delta C_T$ is made for viscous media.

The photostationary trapping efficiency for the direct transport problem in three dimensions can be obtained from the Laplace transform of eq 11

$$1 - M = \frac{\pi\gamma_3 C_T}{2}\exp\left[\frac{\pi(\gamma_3 C_T)^2}{4}\right]\operatorname{erfc}\left[\frac{\pi^{1/2}\gamma_3 C_T}{2}\right] \quad (13)$$

In one and two dimensions, the integration must be carried out numerically.

The trapping problem becomes considerably more complex if the excitations are allowed to migrate among the donor chromophores via a resonance interaction, in addition to the direct transport to traps. Yokota and Tanimoto[34] have formulated an approximate solution to the direct transport problem when the donors can diffuse through the medium. However, this solution cannot be applied when the donor excitations are mobile as a result of resonance interactions. Such interactions are of a long-range nature, and when coupled with statistical fluctuations in chromophore density, they can lead to highly nondiffusive behavior.

Huber[21] has formulated an average t-matrix approximate solution to the transport master equation for interacting donors on a regular lattice with a small concentration of randomly placed traps. He has shown that by retaining only the diagonal elements of the t matrix, an expression for $\tilde{G}^D(s)$ can be obtained that is very similar to the phenomenological hopping model of Burshtein.[35] Huber has also applied a coherent potential approximation[22] to the trapping problem at high trap concentrations. Both Huber and Burshtein have demonstrated that for three-dimensional (3-D) disordered systems interacting through dipole–dipole mechanisms, the effect of allowing excitations to migrate between donors is to exponentialize the long-time decay of $G^D(t)$.

Recently, Loring, Andersen, and Fayer[19] (LAF) have obtained a self-consistent solution to the full trapping problem in random 3-D systems that is accurate over a broad range of concentrations and times. The solution is also valid for any ratio of the interaction radii, R^{DT}/R^{DD}. The solution technique was based on a diagrammatic ex-

pansion of the Green's function for the average density of excitations, similar to the approach taken by Gochanour, Andersen, and Fayer[18] (GAF) for a disordered one-component system. Although the trapping problem was originally solved for dipolar interactions in 3-D, the technique was later extended to multipolar interactions in 1-D and 2-D by Loring and Fayer[20] (LF). For isotropic dipolar transport rates of the form

$$w(r) = k_D\left(\frac{R^{DD}}{r}\right)^6, \quad \text{donor–donor} \tag{14a}$$

$$v(r) = k_D\left(\frac{R^{DT}}{r}\right)^6, \quad \text{donor–trap} \tag{14b}$$

the two-body approximation of LAF for the Laplace transform of $G^D(t)$ in three dimensions is

$$\tilde{G}^D(s) = \frac{[\tilde{G}^S(s)]^2}{\tilde{G}^S(s) - \tilde{\Delta}[\tilde{G}^S(s)]} \tag{15a}$$

where

$$\tilde{\Delta}[\tilde{G}^S(s)] = \frac{\pi}{2^{3/2}} C_D k_D^{1/2} [\tilde{G}^S(s)]^{3/2} \tag{15b}$$

and

$$[\tilde{G}^S(s)]^{1/2} = \frac{1}{2s}\left\{-\left[\frac{\pi}{2}k_D^{1/2}C_T + \frac{\pi}{2^{3/2}}k_D^{1/2}C_D\right] + \left[\left(\frac{\pi}{2}k_D^{1/2}C_T + \frac{\pi}{2^{3/2}}k_D^{1/2}C_D\right)^2 + 4s\right]^{1/2}\right\} \tag{15c}$$

The dimensionless donor and trap concentrations are defined in accordance with eq 10

$$C_D = \tfrac{4}{3}\pi (R^{DD})^3 \rho_D \tag{16a}$$

$$C_T = \tfrac{4}{3}\pi (R^{DT})^3 \rho_T \tag{16b}$$

A more accurate three-body approximation to $\tilde{G}^D(s)$ that exhibits an additional dependence on the ratio R^{DT}/R^{DD} is given by LAF, but for simplicity we omit the expression here. The transient fluorescence response can be obtained very efficiently from eq 15 by numerical transform inversion with the Stehfest algorithm,[36] while the photostationary results are given directly through eq 6.

As in the direct-trapping problem, it can be shown in the LAF and LF two-body approximations that for a viscous solution, the static average of randomly oriented transition dipoles can be taken into account by the replacement (see Appendix B)

$$C_D \rightarrow \gamma_\Delta C_D \tag{17a}$$

$$C_T \rightarrow \gamma_\Delta C_T \tag{17b}$$

It is generally assumed that this substitution will also hold in the three-body approximation,[37] although it has not been demonstrated rigorously.

LAF have shown that transport in the two-component system is nondiffusive by observations of the time behavior of the mean squared displacement and by the fact that the long-time generalized diffusion coefficient is zero. From their results, it is easy to formulate an explicit expression for the Laplace transform of the mean squared displacement in the two-body approximation

$$\langle \tilde{R}^2(s)\rangle = \pi (R^{DD})^2 \{2^{-1/6}C_D + C_T k^2 s \tilde{G}^S(s) + 2^{-7/6}\pi C_D C_T [\tilde{G}^S(s)]^{1/2}[2^{-1/3}k^2 - 1]\}/\{s[\tilde{G}^S(s)]^{1/6}(s + \pi^2 2^{-5/2} C_D C_T)\} \tag{18}$$

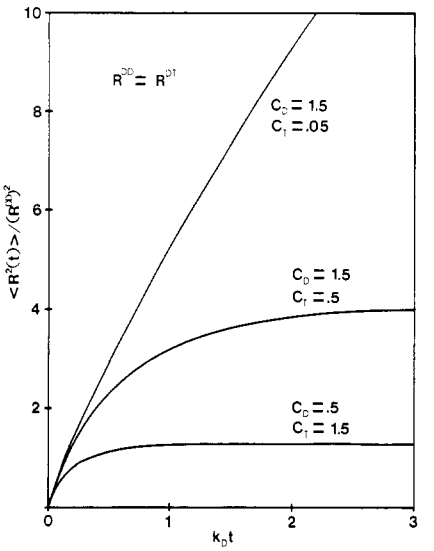

Figure 1. Mean squared displacement as calculated from the LAF model in the two-body approximation, eq 18. $\langle R^2(t)\rangle$ reaches a finite maximum given by eq 20 which is determined by a pair of reduced donor and trap concentrations, C_D and C_T.

where $k \equiv R^{DT}/R^{DD}$ and $\tilde{G}^S(s)$ is given by eq 15c. We have plotted the inverse transform[36] of eq 18 for several donor and trap concentrations in Figure 1. Classical diffusion in three dimensions dictates that $\langle R^2(t)\rangle_{diff} = 6Dt$, but the curves in Figure 1 do not exhibit this linear behavior. The maximum that $\langle R^2(t)\rangle$ attains for a given donor and trap concentration is a measure of the average squared distance an excitation can migrate nondiffusively before being trapped. This leads us to define an "effective migration length" by

$$l = \langle R^2(\infty)\rangle^{1/2} \tag{19}$$

and from eq 18 and the final value theorem for Laplace transforms we obtain

$$l = R^{DD}\left\{\frac{2^{7/3}A^{1/3}}{\pi C_T} + \frac{2(k^2 - 2^{1/3})}{A^{2/3}}\right\}^{1/2} \tag{20a}$$

with

$$A = \frac{\pi}{2}C_T + \frac{\pi}{2^{3/2}}C_D \tag{20b}$$

Equation 20 is the dipole–dipole nondiffusive counterpart of a classical diffusion length in the presence of sinks. Expressions similar to eq 20 can be easily developed for higher order multipole interactions or for systems of lower dimensionality.

We conclude this section with the comment that the models considered thus far are for homogeneous, randomly distributed systems of donors and traps. In contrast, chromophores attached to a chain in a random coil configuration present an anisotropic energy transport pathway. In addition to the nonuniformity of the chromophore distribution, the finite boundaries of an isolated coil may play an important role in determining the time behavior of the trapping process.[28] As a result, it is necessary to develop expressions for $G^D(t)$ appropriate to the variety of morphological conditions found in polymeric systems. Work on this general class of problems is currently in progress.

III. Fluorescence Depolarization Theory

In this paper we only consider the depolarization of fluorescence resulting from resonance transfer and not

from rotational relaxation. Furthermore, the discussion will be restricted to one-component systems, i.e., donors in the absence of traps.

One of the first time-dependent theories of concentration depolarization was formulated by Hemenger and Pearlstein.[38] Their theory, however, was based on a density expansion and thus had the same drawback as earlier steady-state theories[39,40] in that the solution failed at high chromophore concentrations. In contrast, the diagrammatic expansion of the transport Green's function by GAF is accurate over a broad concentration range. Since earlier studies indicated that the vast majority of the retention of polarization comes from the fluorescence of molecules that were initially excited,[38,41] Gochanour[37] has related the parallel and perpendicular fluorescence intensities to the "self" portion of the full Green's function

$$I_{\parallel}(t) = \exp(-k_D t)(1 + 0.8G^S(t)) \quad (21a)$$

$$I_{\perp}(t) = \exp(-k_D t)(1 - 0.4G^S(t)) \quad (21b)$$

$G^S(t)$ represents the configurationally averaged probability that an excitation resides on its site of origin at time t. For disordered, 3-D systems with dipolar interactions, the Laplace transform of $G^S(t)$ is given in the three-body approximation by[37]

$$\tilde{G}^S(s) = \{(\pi\gamma_3 C_D)^2/4)[1 - [1 + (32/(\pi\gamma_3 C_D)^2) \times (s/k_D - 0.1887(\gamma_3 C_D)^2)]^{1/2}] + 4(s/k_D - 0.1887(\gamma_3 C_D)^2)\}/\{4k_D(s/k_D - 0.1887(\gamma_3 C_D)^2)^2\} \quad (22)$$

The orientation factor, γ_3, is crucial for the interpretation of concentration depolarization experiments in rigid media, so it has been included explicitly.

The most useful transient quantity for theoretical purposes is the anisotropy, defined by

$$r(t) = \frac{I_{\parallel}(t) - I_{\perp}(t)}{I_{\parallel}(t) + 2I_{\perp}(t)} \quad (23)$$

or in terms of Green's function

$$\frac{r(t;C_D)}{r(t;0)} = G^S(t) \quad (24)$$

Equation 24 has been normalized by the zero-concentration anisotropy since the theoretical maximum of $^2/_5$ is seldom realized in experiments. Transient depolarization experiments provide an excellent test of a transport theory and can be performed at a single sample concentration. Such experiments have been used to demonstrate that eq 22 is very accurate over a significant concentration range.[37]

Although time-dependent anisotropy data are more desirable, the majority of the available depolarization data for polymeric systems are steady-state measurements of the inverse polarization

$$P^{-1} = (I_{\parallel} + I_{\perp})/(I_{\parallel} - I_{\perp}) \quad (25)$$

The connection between P^{-1} and $G^S(t)$ can be made through the steady-state anisotropy

$$\bar{r} = \int_0^\infty dt\, r(t)I(t) / \int_0^\infty dt\, I(t) \quad (26)$$

where the total intensity, $I(t)$, is proportional to $I_{\parallel}(t) + 2I_{\perp}(t)$. Making use of eq 21 and 24, we obtain

$$\frac{\bar{r}(C_D)}{\bar{r}(0)} = k_D\tilde{G}^S(s = k_D) \quad (27)$$

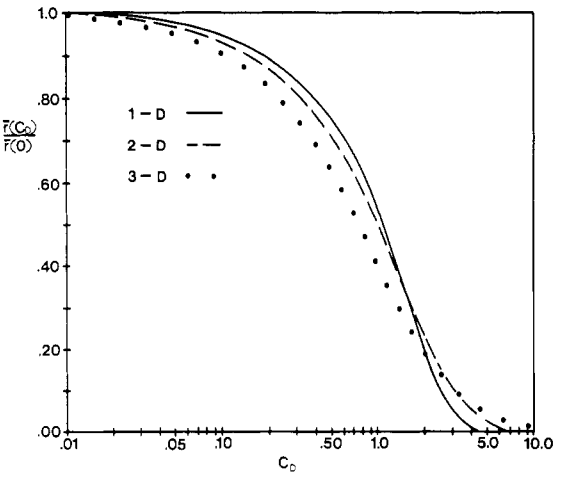

Figure 2. Steady-state anisotropy for a one-component system as a function of reduced concentration. The curves were calculated in the two-body approximation of LAF and LF for transport in one, two, and three dimensions.

Hemenger[38] has shown that for excitation by polarized light, P^{-1} is related to $\bar{r}$ by

$$\bar{r} = {}^2/_3(P^{-1} - {}^1/_3)^{-1} \quad (28)$$

so that the inverse polarization is

$$\frac{P^{-1}(C_D)}{P^{-1}(0)} = \frac{1}{6}\left(1 + \frac{5}{k_D\tilde{G}^S(s = k_D)}\right) \quad (29)$$

Thus, we find that in both trapping and depolarization experiments, the transient observables are directly related to a portion of the full Green's function (i.e., $G^D(t)$ and $G^S(t)$), while the steady-state observables are given in terms of the Laplace transform of these quantities.

As does $G^D(t)$, $G^S(t)$ depends strongly on the dimensionality and chromophore distribution of the experimental system. For one- and two-dimensional disordered one-component systems with dipolar interactions, we have used the two-body self-consistent equation of LF[20] to obtain algebraic equations for $k_D\tilde{G}^S(s = k_D)$. The solution of these equations yields an expression for $\bar{r}(C_D)/\bar{r}(0)$ in the case of randomly oriented, fixed dipoles

$$\bar{r}(C_D)/\bar{r}(0) = [g(C_D)]^6, \quad 1\text{-D} \quad (30a)$$

$$\bar{r}(C_D)/\bar{r}(0) = [h(C_D)]^3, \quad 2\text{-D} \quad (30b)$$

where g and h satisfy

$$g^6 + \left[2^{-5/6}\frac{\pi}{3}(\gamma_1 C_D)\right]g - 1 = 0 \quad (30c)$$

$$h^3 + \left[\frac{2^{1/3}\pi}{3^{3/2}}(\gamma_2 C_D)\right]h - 1 = 0 \quad (30d)$$

The dimensionless concentrations are defined to be consistent with eq 10

$$C_D = 2R^{DD}\rho_D, \quad 1\text{-D} \quad (31a)$$

$$C_D = \pi(R^{DD})^2\rho_D, \quad 2\text{-D} \quad (31b)$$

The steady-state anisotropy has been plotted in Figure 2 for 1-D, 2-D, and 3-D random systems in the two-body approximation as a function of concentration. The 3-D result compares favorably with earlier models in their range of applicability, $C_D \lesssim 1$ (cf. Figure 3 of ref 38). The curves in Figure 2 are extremely useful for experimental analysis since they are universally applicable to dipolar interactions in random, rigid media. It is clear that the onset of de-

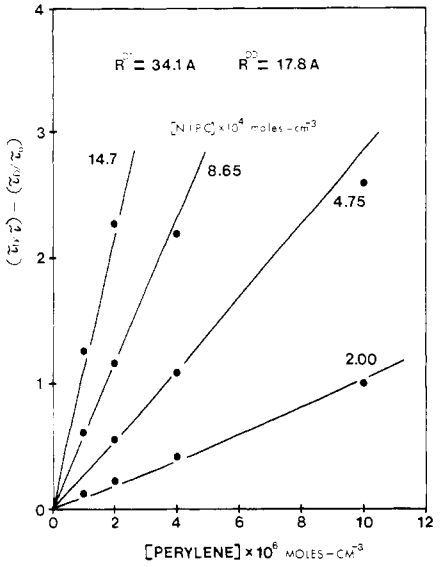

Figure 3. Fit of the three-body LAF model to the lifetime quenching data of Johnson (*Macromolecules* **1980**, *13*, 145) for the NIPC–perylene system. The data were taken from Figure 10 of the paper, and we have corrected the mislabeling of the ordinate in the original figure.

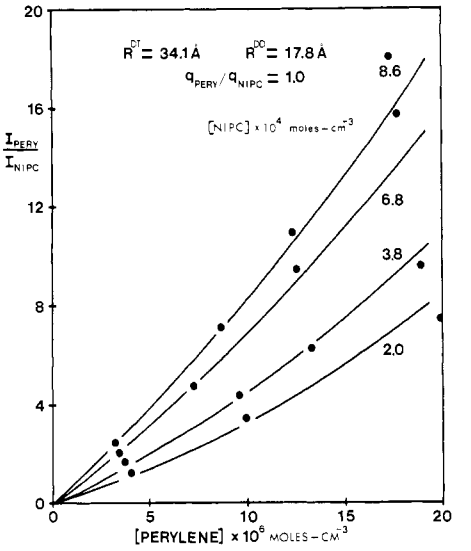

Figure 4. Calculation of the photostationary trap to donor fluorescence intensity ratio as a function of trap concentration. The solid curves were computed with the three-body LAF model using the parameters of Figure 3. The data shown are taken from Figure 6 of Johnson.[42]

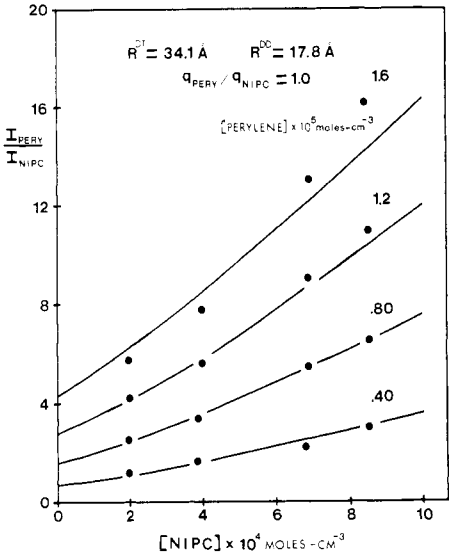

Figure 5. Calculation of the photostationary trap to donor fluorescence intensity ratio as a function of donor concentration. The solid curves were computed with the three-body LAF model using the parameters of Figure 3. The data shown are taken from Figure 7 of Johnson.[42]

polarization is considerably more abrupt for 1-D transport than for 3-D transport. Thus, $\bar{r}$ (or P^{-1}) is sensitive to the dimensionality of energy migration and can be used to draw qualitative conclusions about the dominant transport pathway in polymers of unknown morphology. We will return to this point in section V.

IV. Trapping Experiments in Polymers

As an application of the theory outlined in section II, we have used the 3-D model of LAF to analyze transient and photostationary fluorescence data taken by Johnson[42] for *N*-isopropylcarbazole (NIPC) and perylene in a rigid polystyrene (PS) glass. In this system NIPC serves as an energy donor, while perylene is the energy acceptor. Since the chromophores are not bound to the PS chains, we might expect that a homogeneous transport and trapping model is applicable.

In Figure 3 we have reproduced Johnson's lifetime data for the NIPC–perylene system. The lifetime, τ, represents the time for the nonexponential donor intensity to decay to $1/e$ of its initial value. The quantity τ_0 is this same lifetime when the donor concentration is extrapolated to zero, and τ_D is equal to k_D^{-1}. As a result, an increase in the quantity $\tau_D/\tau - \tau_D/\tau_0$ with donor concentration indicates the presence of donor–donor energy migration.

It is a simple matter to derive an analytical expression for τ_0 from the Förster model. Using eq 11 with $\Delta = 3$, we obtain

$$(\tau_0/\tau_D) = \tfrac{1}{4}[(\pi(\gamma_3 C_T)^2 + 4)^{1/2} - \pi^{1/2}\gamma_3 C_T]^2 \quad (32)$$

The observed lifetime, τ, is obtained by numerical Laplace inversion[36] of the two- or three-body expression for $\tilde{G}^D(s)$ and satisfies the equation

$$\exp(-\tau/\tau_D)G^D(\tau/\tau_D;\gamma_3 C_D;\gamma_3 C_T;R^{DT}/R^{DD}) = e^{-1} \quad (33)$$

From transient data at low donor concentration, Johnson has found $R_0^{DT} = 31$ Å, using a Förster model that differs from the expression presented in section II by the definition of the Förster radius. To be consistent with our eq 8 and 11, we require $R^{DT} = (2/\pi^{1/2}\gamma_3)^{1/3}R_0^{DT}$, or $R^{DT} = 34.1$ Å. Thus, the only unknown required to specify $\tau_D/\tau - \tau_D/\tau_0$ at a given donor and trap concentration is R^{DD}. We have performed a one-parameter fit to the data in Figure 3 with the three-body LAF expression for $\tilde{G}^D(s)$ and found the best-fit parameter to be $R^{DD} = 17.8$ Å. This is in reasonable agreement with the literature value for carbazole to carbazole, $R_0^{DD} = 18.5$ Å.[43] The three-body predictions with these parameters are shown as the solid lines in Figure 3.

Since R^{DD} and R^{DT} are now known for this system, all the fluorescence observables can be *directly computed*. In Figures 4 and 5 we have used the three-body approximation to $\tilde{G}^D(s)$ in conjunction with eq 4 and 6 to calculate directly the photostationary-state intensity ratio, $I_{perylene}/I_{NIPC}$. The curves were scaled to fit Johnson's data by adjusting the quantum efficiency ratio to $q_{FT}/q_{FD} = 1.0$. Figures 4 and 5 demonstrate that the ratio increases nonlinearly with donor and trap concentration, and that the model appears to agree with Johnson's data quite well. At very high concentrations there is some deviation from the model, and we hypothesize that this is a result of

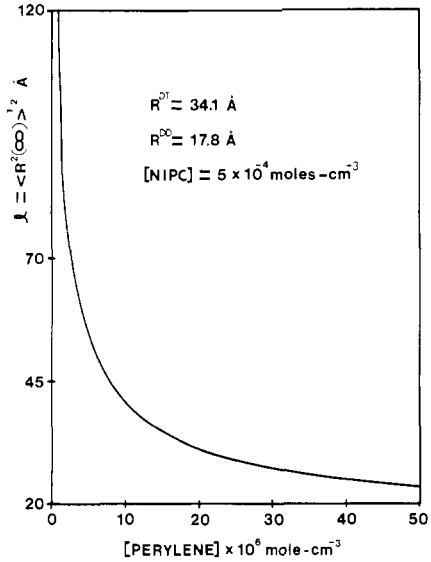

Figure 6. "Effective migration length" plotted against the trap concentration using the parameters of Figure 3 and eq 20.

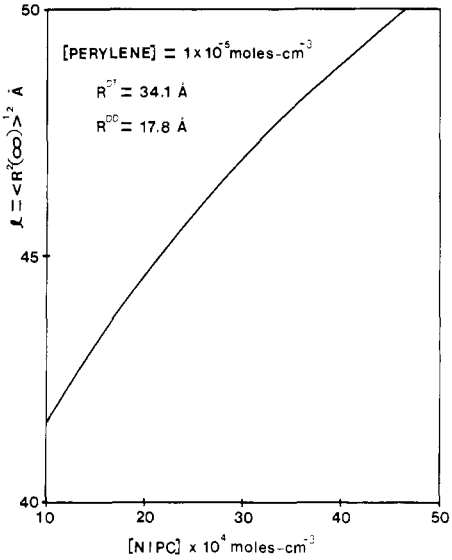

Figure 7. "Effective migration length" plotted against the donor concentration using the parameters of Figure 3 and eq 20.

concentration quenching of the NIPC fluorescence. It is interesting to note that the intercepts of the curves in Figure 5 at [NIPC] = 0 are exactly given by the ratio computed with eq 13. This is a confirmation of the fact that the LAF, three-body model approaches the Förster direct-transport model (eq 11) as $C_D \rightarrow 0$ (see Figure 7, ref 19).

It is a trivial exercise to compute the "effective migration length" for this system as a function of donor and trap concentration. With the substitution $C_D \rightarrow \gamma_3 C_D$ and $C_T \rightarrow \gamma_3 C_T$ in eq 20 and the same interaction radii, we obtain the curves of Figures 6 and 7. The length, l, characterizes the average distance over which an excitation moves in the absence of lifetime decay before being trapped, and from Figure 7 is seen to increase in a nonlinear fashion with donor concentration. Figure 6 demonstrates that l decreases very rapidly with trap concentration and diverges as $C_T \rightarrow 0$.

As a second application of trapping theory we consider a homogeneous system with excimer traps. Trapping at excimer-forming sites (EFS) is a dominant photophysical process in aromatic vinyl polymers, so an understanding of excimer trapping in a simpler, homogeneous system may

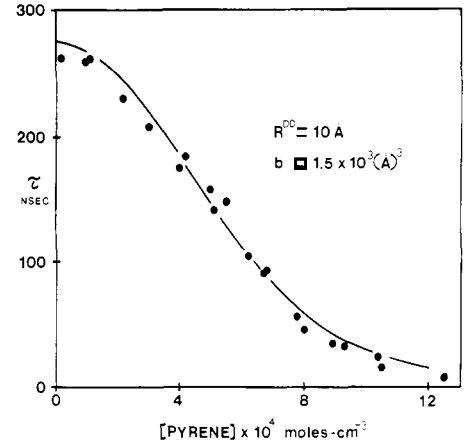

Figure 8. Fit of the three-body LAF model to the lifetime quenching data of Johnson (*Macromolecules* **1980**, *13*, 839) for the pyrene monomer/excimer system. The data were reproduced from Figure 4 of the paper, and the model was applied with the reported value[44] of τ_D = 275 ns.

be useful in the interpretation of experiments with these polymers. First, it is necessary to relate the bulk number density of aromatic chromophores, ρ, to the fraction of chromophores in excimer-forming sites, f_R. For EFS fractions not in the vicinity of one, it is reasonable to assume that a linear relationship exists

$$f_R = b\rho \tag{34}$$

Furthermore, a "trap" is defined as an EFS chromophore pair, so if we assume that the energy transport rate to either member of the pair is the same, the interaction radii are related by

$$R^{DT} = 2^{1/6} R^{DD} \tag{35}$$

Thus, for a 3-D system the dimensionless concentrations are given by

$$C_D = [\tfrac{4}{3}\pi (R^{DD})^3]\rho(1 - b\rho) \tag{36a}$$

$$C_T = [\tfrac{4}{3}\pi (R^{DD})^3]\frac{b}{2^{1/2}}\rho^2 \tag{36b}$$

We selected the pyrene–PS system studied by Johnson[44] for analysis, since the data quality was superior and because the system presents a uniform distribution of an excimer-forming chromophore. The monomer lifetime data of Johnson's Figure 4 are shown in our Figure 8. Using eq 33 and 36, we have fit the data to obtain values for the two unknown parameters, R^{DD} and b. Our best fit yields the values R^{DD} = 10 Å and $b = 1.5 \times 10^3$ Å^3 and is shown as the solid line in Figure 8. The value for τ_D was given by Johnson as 275 ns. We found that it was also possible to describe the data in Figure 8 with the Förster model, eq 32, which indicates that direct trapping is an important process in this system. This result is easily understood, since C_T increases quadratically with pyrene concentration, while C_D increases in a less than linear fashion. The small value of R^{DD} will limit exciton migration until higher concentrations are reached, but concentrated systems contain a large number of traps, causing direct trapping to dominate.

As before, once the unknown transport parameters have been obtained from transient analysis, all the quantities of interest may be directly computed. In Figure 9 we have plotted the ratio of excimer to monomer fluorescence intensities as a function of pyrene concentration. The curve was scaled to fit the data in Johnson's Figure 2 by the quantum efficiency ratio q_{FE}/q_{FM} = 0.30. When photostationary results are generated for excimeric systems, it

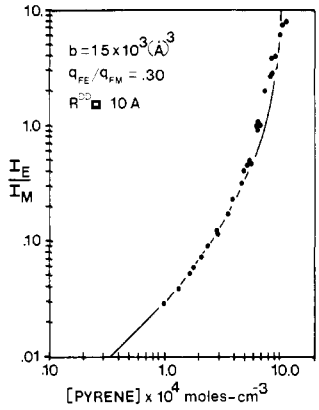

Figure 9. Photostationary-state ratio of excimer to monomer intensity as a function of bulk pyrene concentration. The solid curve was computed with the three-body LAF model using the parameters of Figure 8. The data shown are taken from Figure 2 of Johnson.[44]

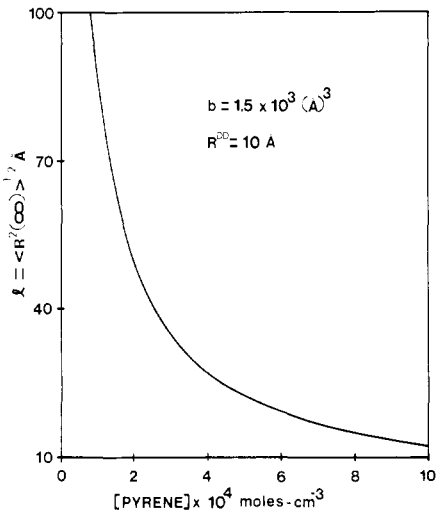

Figure 10. "Effective migration length" plotted against the bulk pyrene concentration using the parameters of Figure 8 and eq 20.

is essential to account for direct absorption onto excimer sites. As a result, eq 6 must be modified to

$$M = (1 - f_R)k_D\tilde{G}^D(s = k_D) \tag{37}$$

In Figure 10 we have plotted the nondiffusive, "effective migration length" for the pyrene–PS system as a function of pyrene concentration. The average distance an excitation can move by a combination of direct transport and migration is seen to decrease rapidly with an increase in bulk concentration.

V. Concentration Depolarization Experiments in Polymers

Although high-resolution transient depolarization studies yield the most accurate information about transport dynamics, very few have been performed on fluorescent polymers. One interesting application of photostationary concentration depolarization, however, is the characterization of copolymers containing both fluorescent and nonfluorescent monomers.[10-17] Such experiments are often done in a low-temperature glass of MTHF, and the polarization data are usually presented as plots of P^{-1} vs. the mole fraction of aromatic monomer, f_a, or vs. the mean aromatic sequence length, $\bar{l}_a$. The energy transport problem for these copolymers is interesting from a fundamental standpoint, since the migrative pathway can exhibit a crossover from three dimensional at low f_a to one

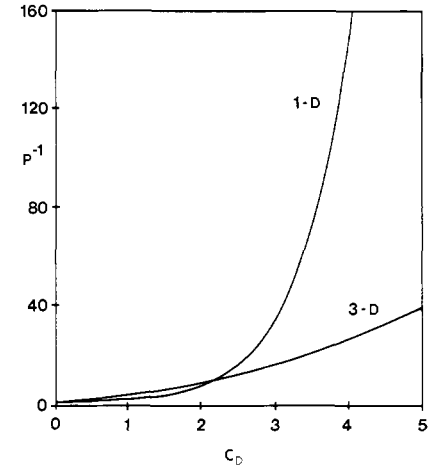

Figure 11. Effect of transport dimensionality on the inverse polarization. The curves were computed with the two-body approximation of LAF (3-D) and LF (1-D).

dimensional at high f_a. Furthermore, such systems may be useful for determining whether the dipole–dipole mechanism is valid for the closely spaced chromophores found along the chain of an aromatic vinyl polymer.

In section III we demonstrated that P^{-1} is simply related to the Laplace transform of $G^S(t)$ for a one-component system. Unfortunately, many of the copolymers studied are capable of forming intramolecular excimer traps between adjacent rings. This enhances the decay of $G^S(t)$ in an unpredictable manner because the excimer trap concentration is usually not known.

$$I_{\parallel}(t) = \exp(-k_D t)G^D(t)(1 + 0.8G^S(t)) \tag{38a}$$

$$I_{\perp}(t) = \exp(-k_D t)G^D(t)(1 - 0.4G^S(t)) \tag{38b}$$

For simplicity we will restrict our consideration to copolymers that are either incapable of excimer formation or have such a low aromatic fraction that excimer formation is very unlikely.

In addition to the dimensional anisotropy induced by the presence of connecting backbone bonds, there is a nonuniform chromophore distribution along the copolymer chain that is determined by the reactivity ratios and feed concentrations of the two monomers. A model for 1-D energy migration on such a chain must account for this distribution. However, for the purpose of making qualitative arguments, we will assume equal reactivity ratios, so that the 1-D, LF model can be applied as the disordered, continuum limit of a Bernoullian lattice of chromophores. In Figure 11 we have recast the 1-D and 3-D $\bar{r}$ curves of Figure 2 on a linear C_D scale in terms of the inverse polarization. The figure indicates that P^{-1} diverges rapidly beyond $C_D \approx 3.0$ for 1-D migration, while the onset of depolarization in 3-D is much more gradual. Thus, it might be expected that P^{-1} data plotted vs. f_a will exhibit a gradual rise for the 3-D migration present at low f_a and then show an abrupt increase when the 1-D concentration rises to about 3. This corresponds to an aromatic mole fraction of

$$f_a \approx \frac{3}{2}\left(\frac{a}{R^{DD}}\right) \tag{39}$$

where a is the average length of a monomer repeat unit. Thus, polymers with large values of the ratio a/R^{DD} may never exhibit the rapid onset of depolarization.

In Figure 12 we have reproduced the P^{-1} data in Table I of David[11] for styrene–methyl acrylate, styrene–methyl methacrylate, and vinylbenzophenone–styrene copolymers.

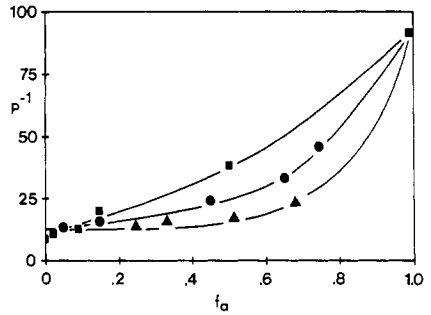

Figure 12. Inverse polarization as a function of the mole fraction of aromatic monomer for copolymers of (●) styrene–methyl acrylate (λ_{ex} = 2600 Å), (▲) styrene–methyl methacrylate (λ_{ex} = 2600 Å), and (■) vinylbenzophenone–styrene (λ_{ex} = 3700 Å). The data are from Table I of David.[11]

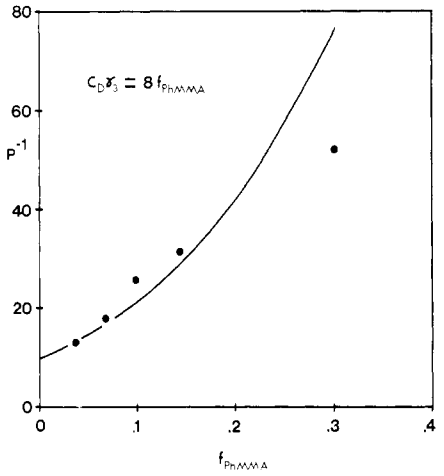

Figure 13. Inverse polarization as a function of the mole fraction of aromatic monomer for the PhMMA–MMA copolymer. The solid curve corresponds to the two-body GAF model for $G^S(t)$ with $\gamma_3 C_D = 8 f_{PhMMA}$. The data are from Figure 5 of Ng and Guillet.[45] $P^{-1}(0)$ was taken as the extrapolated value of 8.0.[45]

These systems show abrupt depolarization at aromatic mole fractions between 0.60 and 0.80. However, this behavior is difficult to quantify since these polymers do contain excimer traps. A system that is void of excimers is the copolymer of (9-phenanthryl)methyl methacrylate (PhMMA) with methyl methacrylate (MMA), studied by Ng and Guillet.[45] In Figure 13 we have reproduced their P^{-1} data, given for aromatic fractions up to 0.30. If R^{DD} is taken to be the literature value of 8.77 Å[43] and $P^{-1}(0)$ is assigned the extrapolated value of 8.0,[45] it is not possible to reproduce the magnitude of depolarization exhibited by the data using the 1-D LF model. Thus, it is reasonable to assume that for this low f_{PhMMA} data, the migrative pathway is esentially 3-D. The solid curve in Figure 13 corresponds to the two-body, 3-D GAF result for $\gamma_3 C_D = 8.0 f_{PhMMA}$. With R^{DD} = 8.77 Å, this corresponds to a local chromophore density of $\rho_D = 3.35 \times 10^{-3} f_{PhMMA}$ Å^{-3}.

VI. Discussion and Conclusions

The excitation dynamics for homogeneous systems of randomly distributed chromophores with well-characterized transport dimensionalities can be adequately modeled by the existing theories of migration and trapping. In polymeric systems with nonuniform chromophore distributions the connection with experimental observables is still made through the quantities $G^S(t)$ and $G^D(t)$, but accurate expressions for the Green's function in nonhomogeneous media are not available. Theoretical analysis should be directed toward obtaining solutions of the Pauli master equation for fundamental morphologies such as isolated coils or concentrated miscible blends. The solutions should be formulated in terms of the full Green's function for the average density of excitations, from which all the transport properties such as $\langle R^2(t) \rangle$ can be obtained. Furthermore, experimental trapping and depolarization studies should be performed on well-characterized systems of a known morphology. Solid solutions or blends are preferable, since they eliminate the additional problem of chromophore diffusion. High-resolution transient experiments yield the most accurate and complete information about excitation dynamics, while photostationary analysis is useful for verifying transport parameters. We anticipate that future improvements in transient apparatus and theoretical developments will make electronic excitation transport an invaluable tool as a quantitative probe of polymer morphology.

Acknowledgment. We thank R. Loring for helpful discussions regarding the application of his theory. This work was supported by the NSF-MRL program administered by the Center for Materials Research at Stanford University.

Appendix A

To compute the orientation factor γ_Δ for random dipoles in a viscous media, we use the result of Blumen[46] to write the exact donor decay law for direct transport to randomly oriented acceptors

$$G^D(t) = \prod_{i=1}^{N}\left[1 - p\left(1 - \frac{\pi^{1/2}}{2}\frac{\text{erf}\,[f_i(t)]}{f_i(t)}\right)\right] \quad \text{(A1)}$$

where

$$f_i(t) = (\tfrac{3}{2}k_D t)^{1/2}(R^{DT}/r_i)^3(1 + 3\cos^2\psi_i)^{1/2}$$

Here, ψ_i is a function that depends only on the direction of the transition dipole of the donor and of the donor–acceptor position. The index i goes over the N lattice sites that the acceptors may occupy with probability p, and r_i represents the distance of separation between the donor and trap i. Equation A1 can be rewritten as[46]

$$G^D(t) = \exp\left(-\sum_{k=1}^{\infty}\left(p^k\frac{S_k(t)}{k}\right)\right) \quad \text{(A2)}$$

where

$$S_k(t) = \sum_{i=1}^{N}\left(1 - \frac{\pi^{1/2}}{2}\frac{\text{erf}\,[f_i(t)]}{f_i(t)}\right)^k \quad \text{(A3)}$$

The summation in eq A3 is replaced by radial and angular integrals in the continuum approximation to yield an expression for $S_k(t)$ in one, two, and three dimensions

$$S_k^1 = 2\rho\int_0^1 dx\int_b^\infty dR\left[1 - \frac{\pi^{1/2}}{2}\frac{\text{erf}\,[f(t)]}{f(t)}\right]^k \quad \text{(A4)}$$

$$S_k^2 = 2\pi\rho\int_0^1 dx\int_b^\infty R\,dR\left[1 - \frac{\pi^{1/2}}{2}\frac{\text{erf}\,[f(t)]}{f(t)}\right]^k \quad \text{(A5)}$$

$$S_k^3 = 4\pi\rho\int_0^1 dx\int_b^\infty R^2\,dR\left[1 - \frac{\pi^{1/2}}{2}\frac{\text{erf}\,[f(t)]}{f(t)}\right]^k \quad \text{(A6)}$$

with

$$f(t) = (\tfrac{3}{2}k_D t)^{1/2}(R^{DT}/R)^3(1 + 3x^2)^{1/2} \quad \text{(A7)}$$

In eq A4–A6, b is a cutoff on the order of the lattice spacing, and ρ is the density of lattice points in the proper

dimension. If the R integration is transformed to integration over $y = \{(^3/_2 k_D t)^{1/2}(R^{DT})^3(1 + 3x^2)^{1/2}\}R^{-3}$, we can take the upper limit on y to infinity in the Förster limit—long times and small b. The result is

$$S_k^1(t) = \frac{2\rho}{3}R^{DT}\left(\frac{3}{2}k_D t\right)^{1/6} I_1\left(\frac{1}{6}\right) I_k^2\left(\frac{4}{3}\right) \quad \text{(A8)}$$

$$S_k^2(t) = \frac{2\pi\rho}{3}(R^{DT})^2\left(\frac{3}{2}k_D t\right)^{1/3} I_1\left(\frac{1}{3}\right) I_k^2\left(\frac{5}{3}\right) \quad \text{(A9)}$$

$$S_k^3(t) = \frac{4\pi\rho}{3}(R^{DT})^3\left(\frac{3}{2}k_D t\right)^{1/2} I_1\left(\frac{1}{2}\right) I_k^2(2) \quad \text{(A10)}$$

where the integrals I_1 and I_k^2 are defined by

$$I_1(q) \equiv \int_0^1 dx\ (1 + 3x^2)^q \quad \text{(A11)}$$

$$I_k^2(q) \equiv \int_0^\infty dy\ y^{-q}\left(1 - \frac{\pi^{1/2}}{2}\frac{\text{erf}\,(y)}{y}\right)^k \quad \text{(A12)}$$

I_1 can be integrated numerically to yield

$$I_1(1/6) = 1.10733 \quad \text{(A13)}$$

$$I_1(1/3) = 1.23288 \quad \text{(A14)}$$

$$I_1(1/2) = 1.38017 \quad \text{(A15)}$$

and for $k = 1$, I_1^2 is easily evaluated by two partial integrations

$$I_1^2\left(\frac{4}{3}\right) = \frac{9}{4}\Gamma\left(\frac{5}{6}\right) \quad \text{(A16)}$$

$$I_1^2\left(\frac{5}{3}\right) = \frac{9}{10}\Gamma\left(\frac{2}{3}\right) \quad \text{(A17)}$$

$$I_1^2(2) = \frac{1}{2}\Gamma\left(\frac{1}{2}\right) \quad \text{(A18)}$$

Thus, by combining eq A8–A18 and retaining only the $k = 1$ term in eq A2, one can obtain the expressions for γ_Δ by comparison with eq 9

$$\gamma_1 = 0.8886 \quad \text{(A19)}$$

$$\gamma_2 = 0.8468 \quad \text{(A20)}$$

$$\gamma_3 = 0.8452 \quad \text{(A21)}$$

It is interesting to note that if the orientation factor, K^2, in the dipolar rate expression[46]

$$v(\vec{r},\vec{\Omega}) = {}^3/_2 K^2(\vec{\Omega}) k_D (R^{DT}/r)^6 \quad \text{(A22)}$$

is expressed in Blumen's notation as

$$K^2(\vec{\Omega}) = (1 + 3\cos^2\psi)\cos^2\theta \quad \text{(A23)}$$

then γ in Δ dimensions can be generated from

$$\gamma_\Delta = [(^3/_2)^{\Delta/6}]{}^1/_4 \int_0^\pi d\psi \sin\psi \int_0^\pi d\theta \sin\theta [K^2(\psi,\theta)]^{\Delta/6} = (^3/_2)^{\Delta/6}\langle (K^2)^{\Delta/6}\rangle \quad \text{(A24)}$$

Appendix B

Equation A24 can also be obtained very easily in the two-body approximations of GAF,[18] LAF,[19] or LF[20] if one recognizes that the inclusion of an independent orientation average for each particle does not affect the diagrammatic algebra. We next observe that the two-body self-energy quantities $\tilde{\Sigma}$, $\tilde{\Delta}$, and $\tilde{\Gamma}$ in Δ dimensions are proportional to $k_D^{\Delta/6}$ for dipolar interactions[18-20] and that the replacement of the isotropic rate, eq 14, by the oriented rate, eq A22, corresponds to the substitution $k_D \rightarrow {}^3/_2 k_D K^2(\vec{\Omega})$. Thus, after both particles are orientation averaged, the self-energy terms are modified by a factor $\gamma_\Delta = (^3/_2)^{\Delta/6}\cdot\langle (K^2)^{\Delta/6}\rangle$. Each self-energy quantity is proportional to a dimensionless concentration C_D or C_T and is related to all the fluorescence observables through the self-consistent equation. Thus, the overall effect of including static orientation averaging in the two-body approximation is the replacement

$$C_D \rightarrow \gamma_\Delta C_D \quad \text{(B1)}$$

$$C_T \rightarrow \gamma_\Delta C_T \quad \text{(B2)}$$

in the expressions for an observable calculated with the isotropic rate, eq 14.

References and Notes

(1) Anufrieva, E. V.; Gotlib, Y. Y. *Adv. Polym. Sci.* **1981**, *40*, 1.
(2) Ghiggino, K.; Roberts, A. J.; Phillips, D. *Adv. Polym. Sci.* **1981**, *40*, 69.
(3) Fitzgibbon, P.; Frank, C. W. *Macromolecules* **1982**, *15*, 733.
(4) Gelles, R.; Frank, C. W. *Macromolecules* **1982**, *15*, 741.
(5) Gelles, R.; Frank, C. W. *Macromolecules* **1982**, *15*, 747.
(6) Gelles, R.; Frank, C. W. *Macromolecules* **1982**, *15*, 1486.
(7) Fitzgibbon, P.; Frank, C. W. *Macromolecules* **1981**, *14*, 1650.
(8) Valeur, B.; Monnerie, L. *J. Polym. Sci., Polym. Phys. Ed.* **1976**, *14*, 11.
(9) Belford, G. G.; Belford, R. L.; Weber, G. *Proc. Natl. Acad. Sci. U.S.A.* **1972**, *69*, 1392.
(10) McNally, I.; Reid, R. F.; Rutherford, H.; Soutar, I. *Eur. Polym. J.* **1979**, *15*, 723.
(11) David, C.; Baeyens-Volant, D.; Geuskens, G. *Eur. Polym. J.* **1976**, *12*, 71.
(12) David, C.; Putman-de Lavareille, N.; Geuskens, G. *Eur. Polym. J.* **1977**, *13*, 15.
(13) David, C.; Baeyens-Volant, D.; Peins, M. *Eur. Polym. J.* **1980**, *16*, 413.
(14) Reid, R. F.; Soutar, I. *J. Polym. Sci., Polym. Lett. Ed.* **1977**, *15*, 153.
(15) Reid, R. F.; Soutar, I. *J. Polym. Sci., Polym. Phys. Ed.* **1978**, *16*, 231.
(16) Anderson, R. A.; Reid, R. F.; Soutar, I. *Eur. Polym. J.* **1980**, *16*, 945.
(17) Reid, R. F.; Soutar, I. *J. Polym. Sci., Polym. Phys. Ed.* **1980**, *18*, 457.
(18) Gochanour, C. R.; Andersen, H. C.; Fayer, M. D. *J. Chem. Phys.* **1979**, *70*, 4254.
(19) Loring, R. F.; Andersen, H. C.; Fayer, M. D. *J. Chem. Phys.* **1982**, *76*, 2015.
(20) Loring, R. F.; Fayer, M. D. *Chem. Phys.* **1982**, *70*, 139.
(21) Huber, D. L. *Phys. Rev. B* **1979**, *20*, 2307.
(22) Huber, D. L. *Phys. Rev. B* **1979**, *20*, 5333.
(23) Haan, S. W.; Zwanzig, R. *J. Chem. Phys.* **1978**, *68*, 1879.
(24) Blumen, A.; Klafter, J.; Silbey, R. *J. Chem. Phys.* **1980**, *72*, 5320.
(25) Godzik, K.; Jortner, J. *J. Chem. Phys.* **1980**, *72*, 4471.
(26) Dexter, D. L. *J. Chem. Phys.* **1953**, *21*, 836.
(27) Fredrickson, G. H.; Frank, C. W. *Macromolecules* **1983**, *16*, 572.
(28) Ediger, M. D.; Fayer, M. D. *J. Chem. Phys.* **1983**, *78*, 2518.
(29) MacCallum, J. R. *Annu. Rep. Prog. Chem., Sect. A: Phys. Inorg. Chem.* **1978**, *75*, 99.
(30) Förster, Th. *Z. Naturforsch, A 1949*, *4*, 321.
(31) Hauser, M.; Klein, U. K. A.; Gösele, U. *Z. Phys. Chem.* **1976**, *101*, 255.
(32) Gösele, U.; Klein, U. K. A.; Hauser, M. *Acta Phys. Chem. Szeged.* **1977**, *23*, 89.
(33) Blumen, A.; Manz, J. *J. Chem. Phys.* **1979**, *71*, 4694.
(34) Yokota, M.; Tanimoto, O. *J. Phys. Soc. Jpn.* **1967**, *22* (3), 779.
(35) Burshtein, A. I. *Sov. Phys.—JETP (Engl. Transl.)* **1972**, *35*, 882.
(36) Stehfest, H. *Commun. Assoc. Comput. Mach.* **1970**, *13*, 47, 624.
(37) Gochanour, C. R.; Fayer, M. D. *J. Phys. Chem.* **1981**, *85*, 1989.
(38) Hemenger, R. P.; Pearlstein, R. M. *J. Chem. Phys.* **1973**, *59*, 4064.
(39) Knox, R. S. *Physica (Utrecht)* **1968**, *39*, 361.
(40) Craver, F. W.; Knox, R. S. *Mol. Phys.* **1971**, *22*, 385.
(41) Jablonski, A. *Acta Phys. Pol. A* **1970**, *38*, 453.
(42) Johnson, G. E. *Macromolecules* **1980**, *13*, 145.
(43) Berlman, I. B. "Energy Transfer Parameters of Aromatic Compounds"; Academic Press: New York, 1973.
(44) Johnson, G. E. *Macromolecules* **1980**, *13*, 839.
(45) Ng, D.; Guillet, J. E. *Macromolecules* **1982**, *15*, 724.
(46) Blumen, A. *J. Chem. Phys.* **1981**, *74*, 6926.